Generation mechanism of a new type of unburnt gas pocket and its influences on the detonation-wave/boundary-layer interaction

DOI:
10.1063/5.0088740

Citation for published version (APA):
Wang, Y., Cai, X., & Mahmoudi Larimi, Y. (2022). Generation mechanism of a new type of unburnt gas pocket and its influences on the detonation-wave/boundary-layer interaction. *Physics of Fluids*, *34*, Article 041704. https://doi.org/10.1063/5.0088740

Published in:
Physics of Fluids

Generation Mechanism of a New Type of Unburnt Gas Pocket and its Influences on the Detonation-wave/Boundary-layer Interaction

Yuqi Wang (王玉奇)[a], Jianhan Liang (梁剑寒)[a,*], Xiaodong Cai (蔡晓东)[a,*], Yasser Mahmoudi[b]

[a] *Science and Technology on Scramjet Laboratory, College of Aerospace Science and Engineering, National University of Defense Technology, Changsha 410073, China*

[b] *Department of Mechanical, Aerospace and Civil Engineering, The University of Manchester, M13 9PL, United Kingdom*

Abstract

This work studies numerically the generation mechanism of a new type of unburnt gas pocket and its effects on the characteristics of detonation-wave/boundary-layer interaction in supersonic flows. Results show that this new type of unburnt pocket is generated due to a local re-ignition of preheated gas behind the separated oblique shocks, unlike the traditional unburnt pockets generated due to the longitudinal instability of the detonation front. The chemical energy released by the new unburnt pocket in the supersonic area is found to be blocked by the shear layer and is unfavorable for the self-sustaining propagation of the detonation wave.

Due to the well-known advantages of detonation combustion over the deflagrative combustion, detonation-based scramjet is believed to achieve significantly improved performance. However, scientific problems regarding the detonation self-sustained propagation in supersonic combustion chambers have gained little focus and thus need to be further investigated. Propagation mechanisms and dynamic features of detonation waves in confined tubes are different from those in free space due to large boundary layer losses and velocity deficits [1-2]. Previous studies have distinguished the detonation flow propagating in quiescent mixtures into the boundary layer flow and the mainstream core flow [4]. The detonation wave propagating in the core flows can result in strong inverse pressure gradient on the tube walls and induces a complicated flow structure, including the boundary layer separation, shock bifurcations, and shear layer instabilities [3], which is the so-called detonation-wave/boundary-layer interaction (DWBLI). The shock interactions may cause local re-ignitions and explosions [5], and the chemical energy released from these re-ignitions can be easily trapped in the vicinity of the walls rather than released to the leading detonation wave [6]. Therefore, the propagation speed of the detonation wave in confined channels has a large deviation from the theoretical Chapman-Jouguet (CJ) detonation speed [7]. Similarly, in supersonic inflows, basic flow structures and detonation propagation mechanisms accord with that in quiescent gases [10,37], except that the boundary layer has developed in advance before the detonation wave passes. It means that the DWBLI could be strengthened and the detonation propagation is more easily influenced by the separation and combustion in the boundary layers. In uniform supersonic flows, experimental analyses demonstrated that the propagation speed of the leading detonation wave in straight tubes is closely related to the ratio of the height occupied by the detonation wave to the height of the duct [8]. While in non-uniform supersonic flows, the self-sustaining mechanism of the detonation propagation becomes more complicated owing to the interaction with a velocity shear layer [9]. Since the combustion mechanisms in the mainstream and boundary layers are totally different owing to shock bifurcations and boundary limit, it is of great importance to distinguish the combustion modes/propagation modes of the detonation wave in the DWBLI [38-40]. Among them, Cai et al. [10] conducted both experiments and simulations to identify the propagation modes of the detonation wave in supersonic flows. In their research, the propagation modes are classified into the oblique shock-induced combustion/Mach stem induced detonation (OSIC/MSID) and the pure oblique shock-induced combustion (OSIC). They found that the propagation mode is mostly determined by the equivalence ratio of the mixtures and large-scale unburnt pockets were also observed behind the oblique shock. It was mentioned in their work that the consumption of these unburnt pockets is promoted by a mixing effect of numerous vortices along the boundary of the unburnt pockets. However, the effects of these large-scale unburnt pockets on the detonation propagation and DWBLI were not investigated in details. In a recent three-dimensional numerical simulation, the detonation propagation mode is found also determined by the inflow Mach number [33].

The phenomenon of unburnt pockets was frequently found to exist in highly unstable detonations [34-35]. The formation of unburnt pockets was summarized basically by two mechanisms [11]; one is based on the longitudinal instability of the detonation front and the other is led by the interactions between the transverse waves. These mechanisms were observed both in detonation structures obtained by two-dimensional and three-dimensional modelling analyses [12-13]. In a recent numerical study [14] it was found that the unburnt pocket can be generated by a pair of hot jets upon collision of two triple points. The formation and consumption of unburnt pockets in a gaseous detonation were also found to be affected by mesh resolutions [15-16]. For low numerical resolutions, the explosion of the unburnt pockets caused by the transverse wave-cutting can be restrained [17], which can lead to failure of the detonation wave propagation. Experimental studies showed that the re-ignition of the unburnt pockets can cause localized explosion and release of considerable amount of energy [18]. If this energy is released upstream of the sonic velocity plane, it supports the self-sustained propagation of the detonation wave [19]. Trajectories of weaker triple points were also found to be caused by the emergence of new transverse waves owing to the re-ignition of the unburnt pockets [20]. However, most of the above numerical studies on unburnt gas pockets were performed under the Eulerian framework. In reality, in supersonic flows the near-wall boundary layers play an important role in determining the formation mechanism of unburnt pockets, as well as the propagation, re-ignition and/or extinction mechanism of the detonation waves [21, 36].

In summary, the phenomenon of unburnt pockets has been studied in previous research, however, their generation mechanisms and influences related to the detonation-wave/boundary-layer interaction have yet to be understood. In the present work, the formation of a new kind of large-scale unburnt pocket in a fuel-lean supersonic mixture is investigated using high-resolution numerical simulations. The interactions of this pocket with the shock structures and detonation propagation are studied in details. The transition mechanisms of the detonation propagation modes resulting from the consumption of this pocket are further analyzed.

In this work, the two-dimensional reactive Navier-Stokes equations are used as the governing equations. A detailed chemical kinetics model with 12 species and 42 elementary reactions [22] is adopted for the calculation of the reactive source term. The detonation structure in unstable detonation have shown to include large-scale vortices which dominate the formation of the turbulent flow [23]. Since these vortices are mostly generated from hydrodynamic instabilities including Kelvin-Helmholtz and Richtmyter-Meshkov instabilities which can be well-solved by two-dimensional analysis [24-25], the present two-dimensional calculations can represent properly the turbulent flow feature of the real detonation wave. The open-source program AMROC (Adaptive Mesh Refinement Object-oriented C++) based on Structured Adaptive Mesh Refinement (SAMR) framework [26] is utilized, which has been high accuracies in solving detonation problems [27]. For numerical scheme, the time-explicit finite volume scheme is used with a CFL number of 0.95. Time-operator splitting method [28] is employed to decouple the transport equations and the reactive source terms. The convective terms of the Navier-Stokes equations are discretized by the second-order accurate MUSCL-TVD upwind scheme. The diffusion terms are discretized by the second-order accurate central difference scheme. The fourth-order accurate semi-implicit GRK4A method [29] is employed for the integration of the stiff reactive source terms caused by detailed chemical kinetics.

The computational domain is set to be a rectangular domain with dimension of $L_x \times L_y = 8cm \times 4cm$. A supersonic $H_2/O_2/N_2$ mixture flows into the region from the right-side boundary. The left-side boundary is set to be an outflow boundary and both of the top and bottom solid wall are set to be no-slip. A Quasi one-dimensional Zel'dovich–von Neumann–Döring (ZND) detonation structure is placed initially at x = 5cm away from the left boundary to initialize the detonation wave. Due to cellular instabilities, the ZND structure then develops into the leading detonation wave interacting with the viscous boundary layer. Previous research

[10] showed that the mixture equivalence ratio (ER) can play an important role in determining the detonation propagation mode. Therefore, two groups of supersonic $H_2/O_2/N_2$ mixtures are considered in this work with different molar ratios (i.e., G1: 0.56:1:2.9 and G2:2:1:2.9), which can represent both of the stable and unstable detonation. To stabilize the position of the DWBLI structure, in both cases, the theoretical CJ speed is utilized as the inflow velocity. It is calculated as 1438m/s and 1931m/s respectively with Cantera [30]. Other flow conditions are initial pressure of 36.1kPa and initial temperature of 581K. The initial base mesh resolution is 320×160 cells. The CJ induction length calculated by Cantera is 2.535mm (group G1), meaning the base grid resolution is about 10 points per induction length (Pts/l_{ig}). To carry out convergence analysis, three different cases of adaptive mesh refinement are implemented as listed in Table 1. Although the axial trajectory of the detonation wave is usually used as the analysis object, it is infeasible in the present work because the detonation wave is almost stationary. Instead, the trajectories of the attachment tip of the first oblique shock are calculated as shown in Fig. 1. It is seen that the calculated propagation of the first oblique shock using the mesh in Case 2 is ahead of that in Case 1. The trajectories in Case 2 and Case 3 are nearly identical. Consequently, the five-level refinement of Case 2 is adopted in the following calculations considering both the computational cost and accuracy.

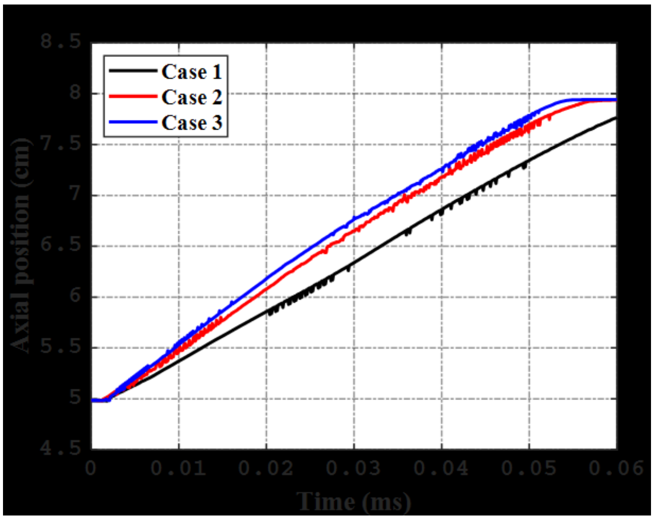

Figure 1. Propagation of the trajectory of the primary separation shock for different mesh resolutions Case1, Case2 and Case 3.

Fig. 2(a) gives a global view about the detonation propagating in supersonic mixtures, including the mainstream detonation wave and the boundary layers. As can be seen, behind the detonation wave front, the streamlines are forced to converge due to the displacement of the separated boundary layers. After the boundary layers reattach back to the solid walls, these streamlines tend to diverge again. Therefore, a hydrodynamic sonic throat is formed behind the detonation wave, which can choke the local flows and cause the overdriven propagation of the detonation wave. Fig. 2(b) illustrates the typical oblique shock-induced combustion/normal shock-induced detonation (OSIC/NSID) structure induced by the DWBLI in details. Owing to the strong inverse pressure gradient exerted by the detonation wave, the boundary layer is separated from the stationary wall and produces a turbulent recirculation zone **RZ**. The separated boundary layer then reattaches to the wall in the downstream with the formation of the reattachment shock **RS**. With the obstruction of the turbulent separated boundary layer, multiple oblique shocks are induced. Here, the first separated oblique shock is named as the primary oblique shock **POS**. When the oblique shock intersects with the leading detonation wave **LD**, the primary triple point **PTP** is generated. To balance the pressure gap passing through the oblique shock and detonation wave, the primary transverse wave **PT** is formed. Meanwhile, the primary shear layer **PSL** is generated behind the primary triple point for discontinuous density and temperature distributions. Vortex structures are induced on this shear layer owing to the Kelvin-Helmholtz (KH) instability to enhance the turbulent mixing. Other mushroom-like vortices are induced by the Richtmyer-Meshkov (RM) instability as well. The strength of the leading detonation wave is unstable with the evolution of cellular structures. The combustion of the incoming gases mostly occurs behind the leading detonation wave for self-sustained propagation. While the gases passing through multiple oblique shocks and the transverse waves (both are oblique shocks) are pre-heated but not consumed. Apart from that, part of the combustion is also induced near the no-slip walls because the flow temperature here is close to the stagnation temperature.

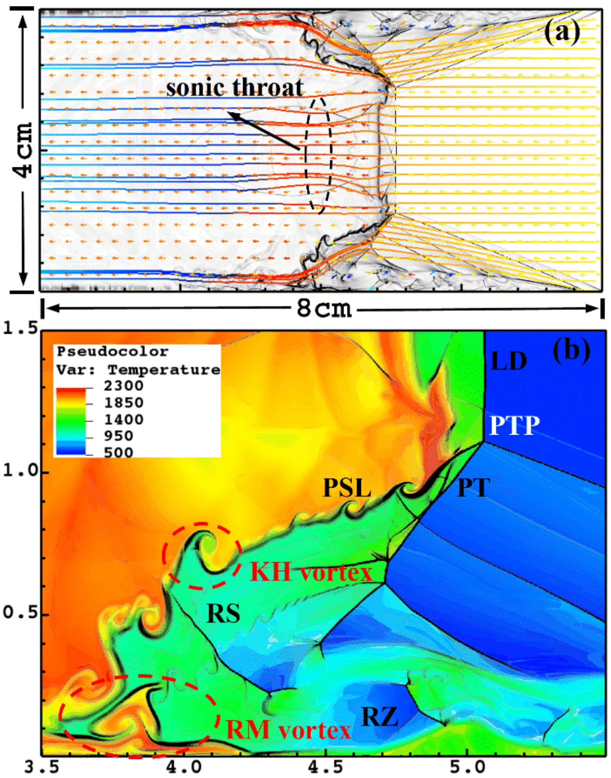

Figure 2. (a) The flow field of the complete domain, (b) Detailed OSIC/NSID Structure induced by the DWBLI.

Table 1. Mesh refinement parameters.

	Case 1	Case 2	Case 3
Refinement level	4 levels (2, 2, 2)	5 levels (2, 2, 2, 2)	6 levels (2, 2, 2, 2, 2)
Points per induction length	Pts / l_{ig} =80	Pts / l_{ig} =160	Pts / l_{ig} =320

As shown in Fig. 3(a), during the evolution of the OSIC/NSID structure, a strong transverse wave travels with the triple point towards the unstable shear layer, producing a high -pressure region. Due to the collision of triple points and reflection, a new transverse wave is reproduced but propagating in an opposite direction with respect to the old one. This reflected transverse wave sweeps the preheated gases again and triggers a local re-ignition, leading to the generation of a weak transverse detonation [31]. The local re-ignition induced in the unreacted mixtures is shown in Fig. 3(b). This re-ignited region is then squeezed along the unstable shear layer in a pair of forward and rearward facing hot jets in Fig. 3(c). As these jets spread, they are affected by a Rayleigh-Taylor instability [12] with their heads gradually developing into a mushroom-like structure. The forward-facing hot jet penetrates deep into the subsonic region behind the local Mach stem, resulting in a stabilized V-shaped flame front. The burning of this jet supports the evolution and enlargement of the local Mach stem, resulting in an induction length similar to that of the mainstream Mach stem. For lack of strong velocity gradient in the longitudinal direction, the rearward-facing jet propagates downstream with a less turbulent front. With the spread of the rearward facing hot jet, the re-ignition region gradually enlarges and eventually links with the burning continents near the wall and behind the mainstream leading detonation wave. Consequently, a new kind of unburnt pocket is produced below the primary shear layer generated from the intersection of the leading detonation wave and primary oblique shock as shown in Fig. 3(d), unlike the traditional unburnt pockets observed behind the leading detonation wave in the previous literature.

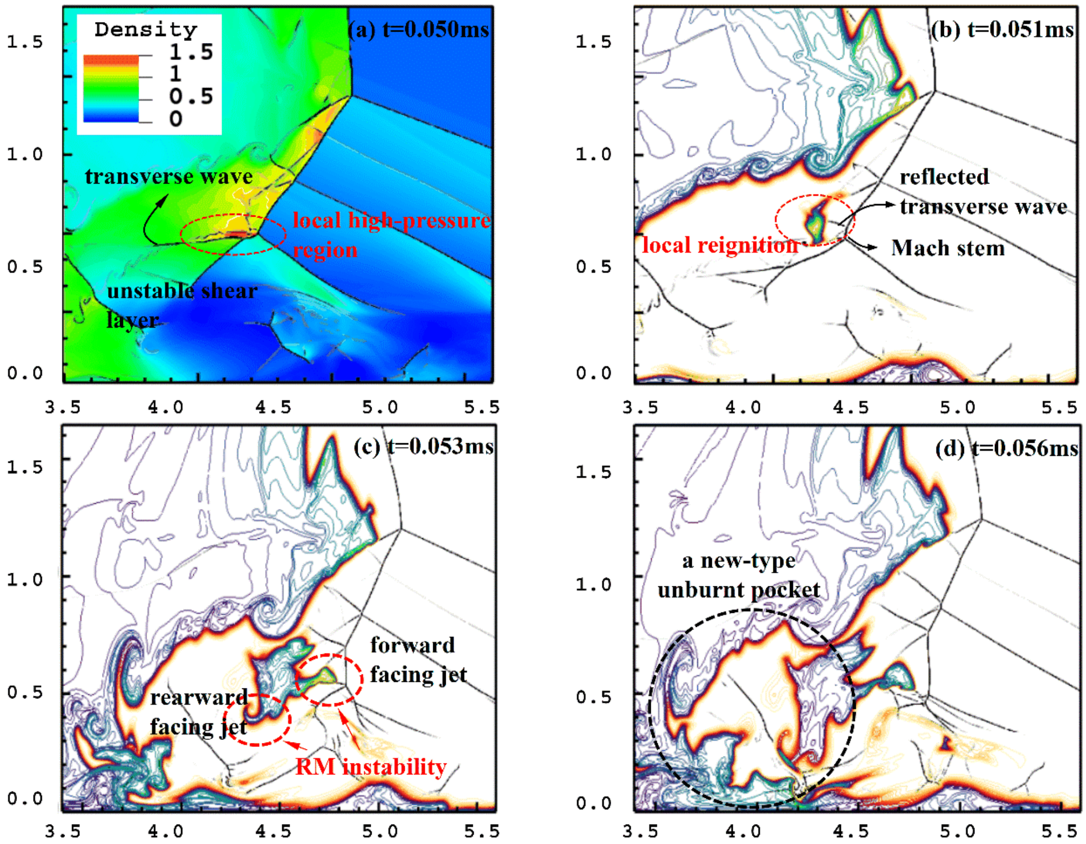

Figure 3. Superposition of (a) density plot and numerical density schlieren illustrating the transverse detonation, (b-d) isolines of OH mass fraction and numerical density schlieren illustrating the formation of the new unburnt pocket.

Above the primary shear layer, the supersonic incoming flow passing through the leading detonation wave becomes subsonic, while the flow below the primary shear layer that passes through the oblique shock remains supersonic. Therefore, the chemical energy released by this pocket in the supersonic area is blocked by the primary shear layer and hard to reach the leading detonation wave. This distinguishes it from traditional unburnt pockets, as the consumption of this new-type unburnt pocket is unfavorable for the self-sustaining propagation of the leading detonation wave. To demonstrate this influence more clearly, group G2 mixture with the ER=1 is further considered as in Fig. 4.

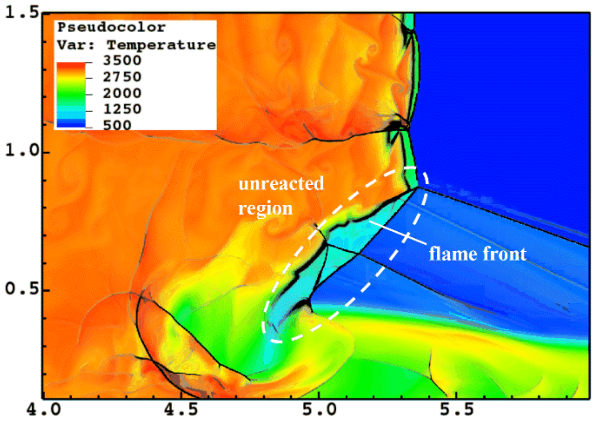

Figure 4. Detailed DWBLI structure in group G2 mixture.

Note that the unburnt gas pocket discussed above is never observed in group G2 mixture during the detonation propagation, demonstrating that this particular phenomenon may be closely related to the equivalence ratio. Although the conditions for the generation of this new-type unburnt gas pocket remain unclear, a brief discussion about the pocket and chemical reactivity of the mixtures is given here. Compared with Fig. 2(b), in Fig. 4 the flame front is pretty close to the primary transverse wave due to higher chemical reactivity, forming a shock-induced combustion structure. The unreacted region is so narrow that gases passing through the oblique shock system and the primary transverse wave are quickly consumed. Therefore, there is no chance for shock interactions or transverse wave reflections to produce a local re-ignition and thus an unburnt gas pocket as observed in fuel-lean mixtures. Further investigations need to be done in the future in finding quantitative relationships between the ER and the generation or size of the unburnt gas pockets. The overdrive degree (u/u_{CJ}) for the detonation front on the centerline is compared in these two group mixtures in Fig. 4(a). It is found that the overdrive degree for the central leading detonation wave in group G2 is basically higher than that in group G1. This is because the boundary layers in G2 are displaced much deeper into the mainstream flow and flows behind the detonation wave are further choked. Due to the thermal instability mechanism [32], prior to group G1 mixture, the overdrive degree in group G2 mixture with higher degree of chemical reactivity shows periodic fluctuations for cellular detonation structures. For G1, one may expect a rebound of the overdrive degree between t=0.045ms and t=0.055ms because of triple point collisions and reflections on the leading detonation wave, similar to that in group G2. Instead, it shows a long declining stage, which corresponds exactly to the time when the unburnt gas pocket forms. Therefore, it can be verified that the formation and consumption of the gas pocket weakens the evolution of the leading detonation wave in group G1.

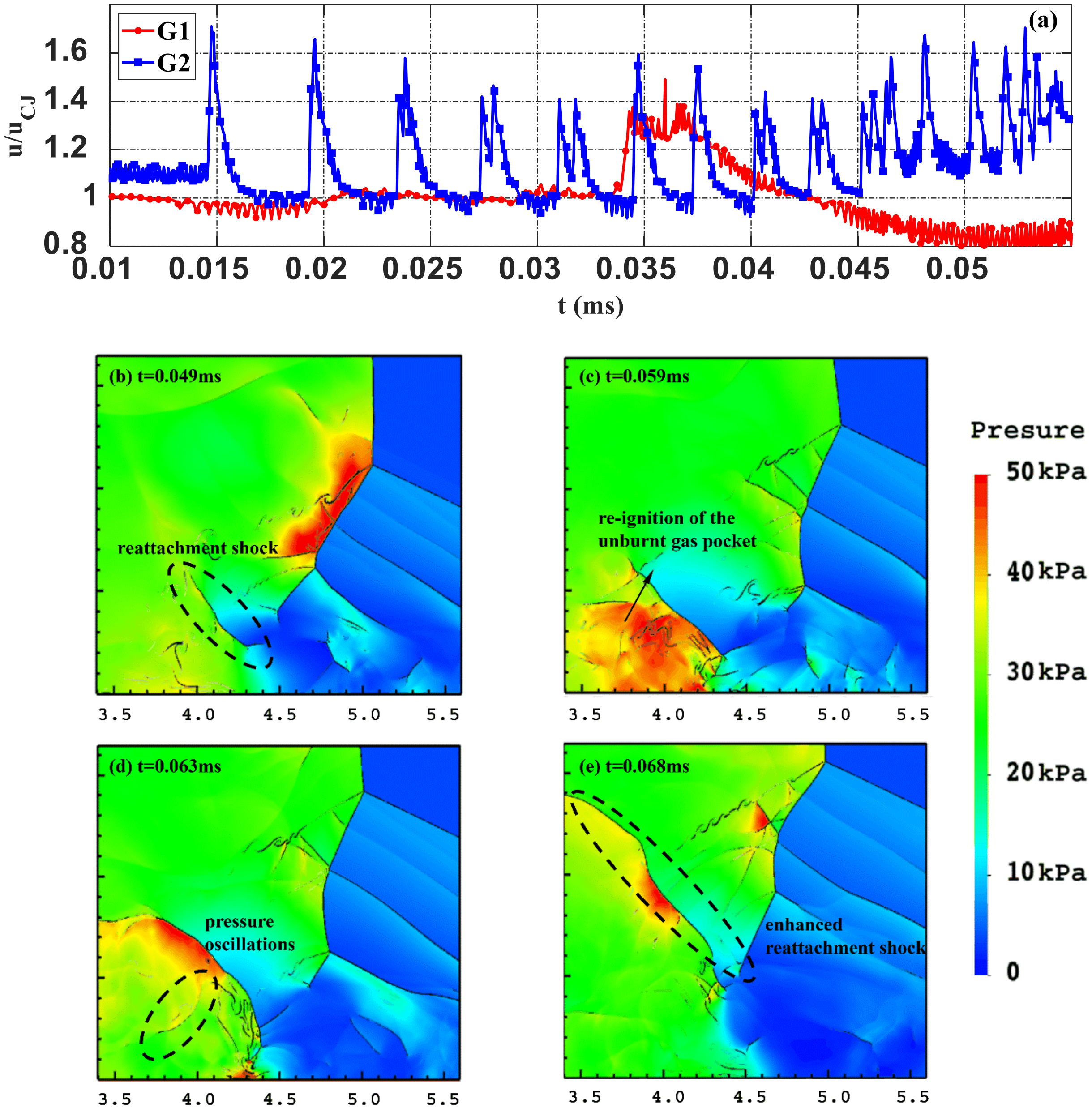

Figure 5. (a) Comparisons of the overdrive degree between group G1 and G2, (b-e) The evolution of pressure plots illustrating the consumption of the squeezed unburnt pockets and the enhancement of the reattachment shock.

In group G1, the reaction rate of the unburnt gas pocket is dramatically increased after passing through the downstream reattachment shock as shown in Fig. 5(b-e). In return, the chemical energy released enhances the strength of the reattachment shock, which further enhances the combustion of the unburnt pocket. This coupled flame-shock consumption mechanism is quite different from the traditional diffusion or turbulent mixing, which makes the pocket consumed much faster. As seen in Figs. 5(d-e) the shock angle of the reattachment shock is highly increased with the generation of pressure and velocity oscillations from the re-ignition of the unburnt gas pocket. These oscillations propagate upstream in the separated boundary layer and greatly enhance the turbulent flow in the recirculation zone with large-scale vortices generated at several spots in Fig. 6. With the promotion of pressure rise and strong turbulence, the combustion induced near the adiabatic wall is further enhanced, resulting to the expansion of the recirculation zone and enhancement of the primary oblique shock in Fig. 6(c). This accelerates the propagation of the oblique shock and further narrows the height occupied by the leading detonation wave in the duct. As a result, the leading detonation wave will disappear for the merging of the two primary oblique shocks eventually in this specific equivalence ratio, and the transition of the propagation modes from the oblique shock-induced combustion/normal shock-induced detonation (OSIC/NSID) to the pure oblique shock-induced combustion (OSIC) is considerably promoted by the consumption of the unburnt gas pocket.

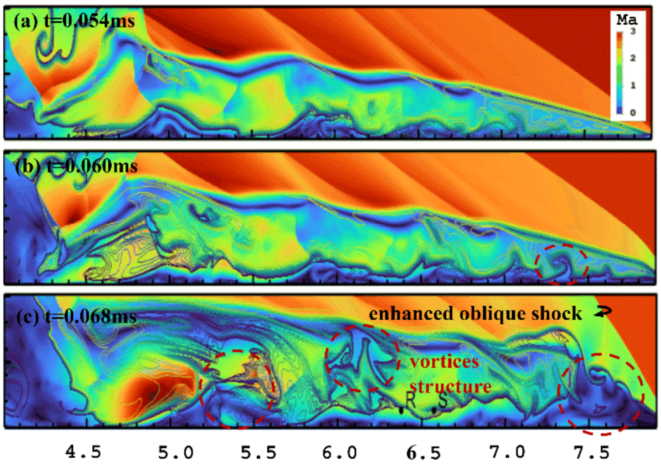

Figure 6. (a-c) The evolution of Mach number plots superimposed by isolines of OH mass fraction illustrating the influences to the separated boundary layer and primary oblique shock.

In this Letter, the two-dimensional reactive Navier-Stokes equations are solved to investigate the problem of detonation-wave/boundary-layer interaction (DWBLI) and explore a new mechanism of formation of unburnt gas pockets. By analyzing the unsteady detonation propagation of a premixed fuel-lean hydrogen-oxygen-nitrogen mixture in details, the generation mechanisms of a new type of unburnt gas pocket are revealed. Unlike traditional unburnt pockets, this pocket is produced below the primary shear layer generated by the intersection of the leading detonation wave and separated oblique shock, owing to the re-ignition triggered by a transverse detonation wave. Quantified analysis indicates that the overdrive degree of the leading detonation wave is reduced because the chemical energy released from the unburnt gas pocket is trapped below the primary shear layer rather than sustaining the leading detonation wave. Instead, the consumption of this pocket influences the DWBLI by enhancing the separated oblique shock and turbulent boundary layers, in the form of pressure and velocity fluctuations propagating upstream in the subsonic boundary-layer flows. Further on, modes transition of detonation propagation from the oblique shock-induced combustion/normal shock-induced detonation (OSIC/NSID) mode to the pure oblique shock-induced combustion (OSIC) mode is thus accelerated. Therefore, the transition mechanism of detonation propagation mode in specific equivalence ratio is partially revealed and explained by studying the new-type unburnt gas pocket. And futural work needs to be done for more essential relationships between the equivalence ratio and this pocket.

Acknowledgement

This work was supported by the National Natural Science Foundation of China (No. 11702323).
The authors have no conflicts to disclose.

Data availability

The data that support the findings of this study are available from the corresponding author upon request.

References

[1] Q. Xiao, A. Sow, B. M. Maxwell, and M. I. Radulescu, “Effect of boundary layer losses on 2D detonation cellular structures,” Proc. Combust. Inst 38 (3), 3641 (2021).

[2] Q. Xiao, and C. Weng, “Effect of losses on hydrogen–oxygen–argon detonation cell sizes,” Phys. Fluids 33 (11), 116103 (2021).

[3] A. A. Vasil’ev, V. A. Vasiliev, A. V. Trotsyuk, “Bifurcation structures in gas detonation,” Combust. Explo. Shock+ 46 (2), 196 (2010).

[4] S. B. Murray, “Numa Manson on velocity deficits and detonation stability,” Shock Waves 18 (4), 255 (2008).

[5] J. Austin, F. Pintgen, and J. Shepherd, “Reaction zones in highly unstable detonations,” Proc. Combust. Inst 30 (2), 1849 (2005).

[6] A. Chinnayya, A. Hadjadj, and D. Ngomo, “Computational study of detonation wave propagation in narrow channels,” Phys. Fluids 25 (3), 036101 (2013).

[7] Vasil’ev, V. Vasiliev, and A. Trotsyuk, “Bifurcation structures in gas detonation,” Combust. Explo. Shock+ 46 (2), 196 (2010).

[8] X. Han, “Investigations on the initiation and propagation mechanism of detonation wave in supersonic premixed gas,” Ph.D. thesis. National University of Defense Technology (2013).

[9] J. Dai, F. Xu, X. Cai, and Y. Mahmoudi, “Effects of velocity shear layer on detonation propagation in a supersonic expanding combustor,” Phys. Fluids 33 (10), 105110 (2021).

[10] X. Cai, J. Liang, R. Deiterding, Y. Mahmoudi, and M. Sun, “Experimental and numerical investigations on propagating modes of detonations: Detonation wave/boundary layer interaction,” Combust. Flame 190, 201 (2018).

[11] M. Sabzpooshani, and K. Mazaheri, “Formation of unburnt pockets in gaseous detonations,” Combust. Explo. Shock+ 45 (2), 182 (2009).

[12] G. J. Sharpe, “Transverse waves in numerical simulations of cellular detonations,” J. Fluid Mech. 447, 31 (2001).

[13] V. Deledicque, and M. V. Papalexandris, “Computational study of three-dimensional gaseous detonation structures,” Combust. Flame 144 (4), 821 (2006).

[14] Y. Mahmoudi, K. Mazaheri, and S. Parvar, “Hydrodynamic instabilities and transverse waves in propagation mechanism of gaseous detonations,” Acta Astronaut 91, 263 (2013).

[15] Y. Mahmoudi, and K. Mazaheri, “High resolution numerical simulation of the structure of 2-D gaseous detonations,” Proc. Combust. Inst 33 (2), 2187 (2011).

[16] K. Mazaheri, Y. Mahmoudi, and M. I. Radulescu, “Diffusion and hydrodynamic instabilities in gaseous detonations,” Combust. Flame 159 (6), 2138 (2012).

[17] J. H. Lee, The Detonation Phenomenon, Cambridge University Press (2008).

[18] M. Radulescu, G. Sharpe, J. Lee, C. Kiyanda, A. Higgins, and R. Hanson, “The ignition mechanism in irregular structure gaseous detonations,” Proc. Combust. Inst 30 (2), 1859 (2005).

[19] A. R. Kasimov, D. S. Stewart, “On the dynamics of self-sustained one-dimensional detonations: A numerical study in the shock-attached flame,” Phys. Fluids 16 (10), 3566 (2004).

[20] E. S. Oran, J. W. Weber Jr, E. I. Stefaniw, M. H. Lefebvre, and J. D. Anderson Jr, “A numerical study of a two-dimensional H2-O2-Ar detonation using a detailed chemical reaction model,” Combust. Flame 113 (1-2), 147 (1998).

[21] Y. Fang, Z. Zhang, Z. Hu, “Effects of boundary layer on wedge-induced oblique detonation structures in hydrogen-air mixtures,” Int. J. Hydrogen Energy 44(41), 23429 (2019).

[22] K. Westbrook, “Chemical kinetics of hydrocarbon oxidation in gaseous detonations,” Combust. Flame 46, 191 (1982).

[23] E. S. Oran, and V. N. Gamezo, “Origins of the deflagration-to-detonation transition in gas-phase combustion,” Combust. Flame 148 (1-2), 4 (2007).

[24] V. N. Gamezo, T. Ogawa, and E. S. Oran, “Numerical simulations of flame propagation and DDT in obstructed channels filled with hydrogen–air mixture,” Proc. Combust. Inst 31 (2), 2463 (2007).

[25] X. Li, and Q. Zhang, “A comparative numerical study of the Richtmyer-Meshkov instability with nonlinear analysis in two and three dimensions,” Phys. Fluids 9 (10), 3069 (1997).

[26] M. J. Berger, and J. Oliger, “Adaptive mesh refinement for hyperbolic partial differential equations,” J. Comput. Phys. 53 (3), 484 (1984).

[27] R. Deiterding, “Parallel adaptive simulation of multi-dimensional detonation structures,” Ph.D. thesis. Brandenburg University of Technology (2003).

[28] N. N. Janenko, Die Zwischenschrittmethode zur Losung mehrdimensionaler Probleme der mathematischen Physik, Springer-Verlag, Berlin (1969).

[29] P. Kaps and P. Rentrop, “Generalized Runge-Kutta methods of order four with stepsize control for stiff ordinary differential equations,” Num. Math. 33 (1), 55 (1979).

[30] Goodwin, and D. Cantera, “Object-Oriented Software for Reacting Flows,” http://www.cantera.org (2002).

[31] R. A. Strehlow, and A. J. Crooker, “The structure of marginal detonation waves,” Acta Astronaut 1 (3-4), 303 (1974).

[32] N. M. Kuznetsov, and V. A. Kopotev, “Detonation in a relaxing gas and relaxational instability,” Combust. Explo. Shock+ 22 (5), 563 (1986).

[33] W. Chen, J. Liang, X. Cai, and Y. Mahmoudi, “Three-dimensional simulations of detonation propagation in circular tubes: Effects of jet initiation and wall reflection,” Phys. Fluids 2(4), 046104 (2020).

[34] M. Reynaud, F. Virot, A. Chinnayya, “A computational study of the interaction of gaseous detonations with a compressible layer,” Phys. Fluids 29(5), 056101 (2017).

[35] W. Han, J. Huang, C. Wang, “Pulsating and cellular instabilities of hydrogen–oxygen detonations with ozone sensitization,” Phys. Fluids 33(7), 076113 (2021).

[36] K. Wu, S. Zhang, D. She, and J. Wang, “Analysis of flow-field characteristics and pressure gain in air-breathing rotating detonation combustor,” Phys. Fluids 33(12), 126112 (2021).

[37] V. N. Gamezo, A. M. Khokhlov, E. S. Oran, “The influence of shock bifurcations on shock-flame interactions and DDT,” Combust. Flame 126 (4), 1810 (2001).

[38] K. P. Grogan, M. Ihme, “Regimes describing shock boundary layer interaction and ignition in shock tubes,” Proc. Combust. Inst 36 (2), 2927 (2017).

[39] Y. Liu, J. Yin, Z. Wang, “Study on the overdriven detonation wave propagation in double-layer shaped charge,” Phys. Fluids 31 (9), 092110 (2019).

[40] D. Zhang, X. Yuan, S. Liu, et al, “Numerical study of detonation wave propagation modes in annular channels,” AIP Adv. 11(8), 085203 (2021).